the FEBS Journal

Processing, catalytic activity and crystal structures of kumamolisin-As with an engineered active site

Ayumi Okubo[1]*, Mi Li[2,3]*, Masako Ashida[1], Hiroshi Oyama[4], Alla Gustchina[2], Kohei Oda[4], Ben M. Dunn[5], Alexander Wlodawer[2] and Toru Nakayama[1]

1 Department of Biomolecular Engineering, Graduate School of Engineering, Tohoku University, Sendai, Japan
2 Protein Structure Section, Macromolecular Crystallography Laboratory, National Cancer Institute at Frederick, MD, USA
3 Basic Research Program, SAIC-Frederick, National Cancer Institute at Frederick, MD, USA
4 Department of Applied Biology, Faculty of Textile Science, Kyoto Institute of Technology, Japan
5 Department of Biochemistry and Molecular Biology, University of Florida, Gainesville, FL, USA

Keywords
active site; autolysis; catalytic mechanism; serine proteases

Correspondence
T. Nakayama, Department of Biomolecular Engineering, Graduate School of Engineering, Tohoku University, 6-6-11, Aoba-yama, Sendai 980-8579, Japan
Fax/Tel: +81 22 795 7270
E-mail: nakayama@seika.che.tohoku.ac.jp

*These authors contributed equally to this work

(Received 23 February 2006, revised 31 March 2006, accepted 10 April 2006)

doi:10.1111/j.1742-4658.2006.05266.x

Kumamolisin-As is an acid collagenase with a subtilisin-like fold. Its active site contains a unique catalytic triad, Ser278-Glu78-Asp82, and a putative transition-state stabilizing residue, Asp164. In this study, the mutants D164N and E78H/D164N were engineered in order to replace parts of the catalytic machinery of kumamolisin-As with the residues found in the equivalent positions in subtilisin. Unlike the wild-type and D164N proenzymes, which undergo instantaneous processing to produce their 37-kDa mature forms, the expressed E78H/D164N proenzyme exists as an equilibrated mixture of the nicked and intact forms of the precursor. X-ray crystallographic structures of the mature forms of the two mutants showed that, in each of them, the catalytic Ser278 makes direct hydrogen bonds with the side chain of Asn164. In addition, His78 of the double mutant is distant from Ser278 and Asp82, and the catalytic triad no longer exists. Consistent with these structural alterations around the active site, these mutants showed only low catalytic activity (relative k_{cat} at pH 4.0 1.3% for D164N and 0.0001% for E78H/D164N). pH-dependent kinetic studies showed that the single D164N substitution did not significantly alter the logk_{cat} vs. pH and log(k_{cat}/K_m) vs. pH profiles of the enzyme. In contrast, the double mutation resulted in a dramatic switch of the logk_{cat} vs. pH profile to one that was consistent with catalysis by means of the Ser278-His78 dyad and Asn164, which may also account for the observed ligation/cleavage equilibrium of the precursor of E78H/D164N. These results corroborate the mechanistic importance of the glutamate-mediated catalytic triad and oxyanion-stabilizing aspartic acid residue for low-pH peptidase activity of the enzyme.

The sedolisin family of proteolytic enzymes (now identified in the MEROPS database [1] as S53) was initially known as pepstatin-insensitive acid peptidases [2,3]. However, recent crystallographic and modeling studies revealed that the sedolisins (sedolisin, kumamolisin, kumamolisin-As, and CLN2) have an overall fold that is very similar to that of subtilisin [4–8]. The active sites of these enzymes contain a unique catalytic triad, Ser-Glu-Asp, in place of the canonical Ser-His-Asp triad of the classical serine peptidases. In the latter case, the Ser and His residues act as nucleophilic and general acid/base catalysts, respectively [9,10]. The Asp residue of the catalytic triad of sedolisins, although conserved in its nature, originates from a different part

Abbreviations
IQF, internally quenched fluorogenic.

of the structure compared with the Asp residue of classical serine peptidases and is thus topologically different. Moreover, sedolisins contain an Asp residue in the 'oxyanion hole', which replaces Asn155 of the classical subtilisin-like proteases [11]. The role of that structural element, which is not actually a true cavity in either subtilisins or sedolisins, is to stabilize the negative charge that develops during cleavage of the peptide bond. These structural observations strongly suggest that sedolisins are essentially serine peptidases, and the occurrence of a glutamic acid residue in their catalytic triad, as well as of an aspartic acid residue in the oxyanion hole, must be closely related to the preference of their catalytic activity for acidic pH. Moreover, recent biochemical and crystallographic studies have provided strong evidence that mature forms of these enzymes are produced from their precursors by intramolecular cleavage [12,13].

Kumamolisin-As is a recently discovered member of the sedolisin family, identified by Tsuruoka *et al.* in the culture filtrate of a thermoacidophilic soil bacterium *Alicyclobacillus sendaiensis* strain NTAP-1 and initially named ScpA [14,15]. It is the first known example of an acid collagenase from the sedolisin family. It is encoded as a 57-kDa precursor protein consisting of an N-terminal prodomain [15] (Met1p-Ala189p; residue numbers of the prodomain are designated with the suffix 'p') and a catalytic domain (Ala1-Pro364; residues in the mature catalytic domain are numbered without a suffix where unambiguous, and with the suffix 'e' otherwise) (Fig. 1). We have previously determined the crystal structure of the mature form of this enzyme to clarify the structural basis for the preference of the enzyme for collagen [7]. As in kumamolisin, the catalytic triad of kumamolisin-As is formed from Ser278, Glu78, and Asp82. The side chains of these residues are connected by short hydrogen bonds which are extended out to two additional residues, Glu32 and Trp129 [6,7]. The oxyanion hole is created in part by the side chain of Asp164. The structure of the E78H mutant was also solved previously and compared with that of the wild-type enzyme [7]. In the work presented here, the mutagenesis studies were designed to bring the pH optimum of kumamolisin-As closer to the optima found for the subtilisins, by engineering the mutants D164N and E78H/D164N. X-ray crystallographic analyses of these mutants revealed that they have altered hydrogen-bond networks in their active site and, consistent with these observations, exhibit low enzyme activities. Specifically, the E78H/D164N mutant displayed significantly altered behavior with respect to the processing of its precursor and the pH-dependent kinetics, which appeared to be mediated by the Ser278-His78 dyad and by Asn164. The results, in turn, corroborate the mechanistic importance of the glutamate-mediated catalytic triad and an aspartic acid residue in the oxyanion hole of sedolisins for their low-pH peptidase activity.

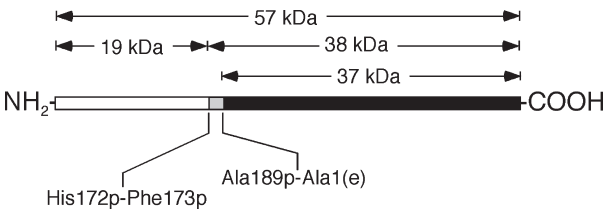

Fig. 1. Schematic representation of the structure of the precursor of kumamolisin-As, consisting of an N-terminal propeptide (white rectangle), the linker part (gray rectangle), and the mature form of the enzyme (black rectangle). Sizes of the related cleavage products are those estimated from the deduced amino-acid sequences and are shown with double-headed arrows. Cleavage sites are shown below the rectangle.

Results

Processing and purification of mutants

The D164N and E78H/D164N mutants were overexpressed in *Escherichia coli* cells under the control of the T7 promoter. The E78A/D164N and E78Q/D164N mutants were also created to compare their properties with those of E78H/D164N. All of these single and double mutants of kumamolisin-As were produced as soluble proteins.

The expressed D164N mutant was identified in its 37-kDa mature form in the crude extract (before heat treatment) and purified to homogeneity (Fig. 2A) after heat treatment (at pH 4.0 and 55 °C for 3 h), followed by anion-exchange chromatography at pH 7.0, as in the case of the wild-type enzyme (Fig. 2A) [7,15].

In contrast, SDS/PAGE of the crude extract of transformant cells overexpressing the E78H/D164N mutant showed that the expressed product gave two major protein bands with molecular masses of 38 kDa and 19 kDa (Fig. 2A), along with a small amount of its 57-kDa precursor form, each identified by automated Edman degradation (five cycles). The stoichiometry of these 38-kDa and 19-kDa proteins was determined by scanning densitometry of Coomassie blue-stained bands in the SDS/polyacrylamide gel and appeared to be 1 : 1, after normalization for molecular mass. The N-terminal amino-acid sequences of these major proteins were Phe-Arg-Met-Gln-Arg- for the 38-kDa species and Ser-Asp-Met-Glu-Lys- for the 19-kDa species, strongly suggesting that respective protein bands

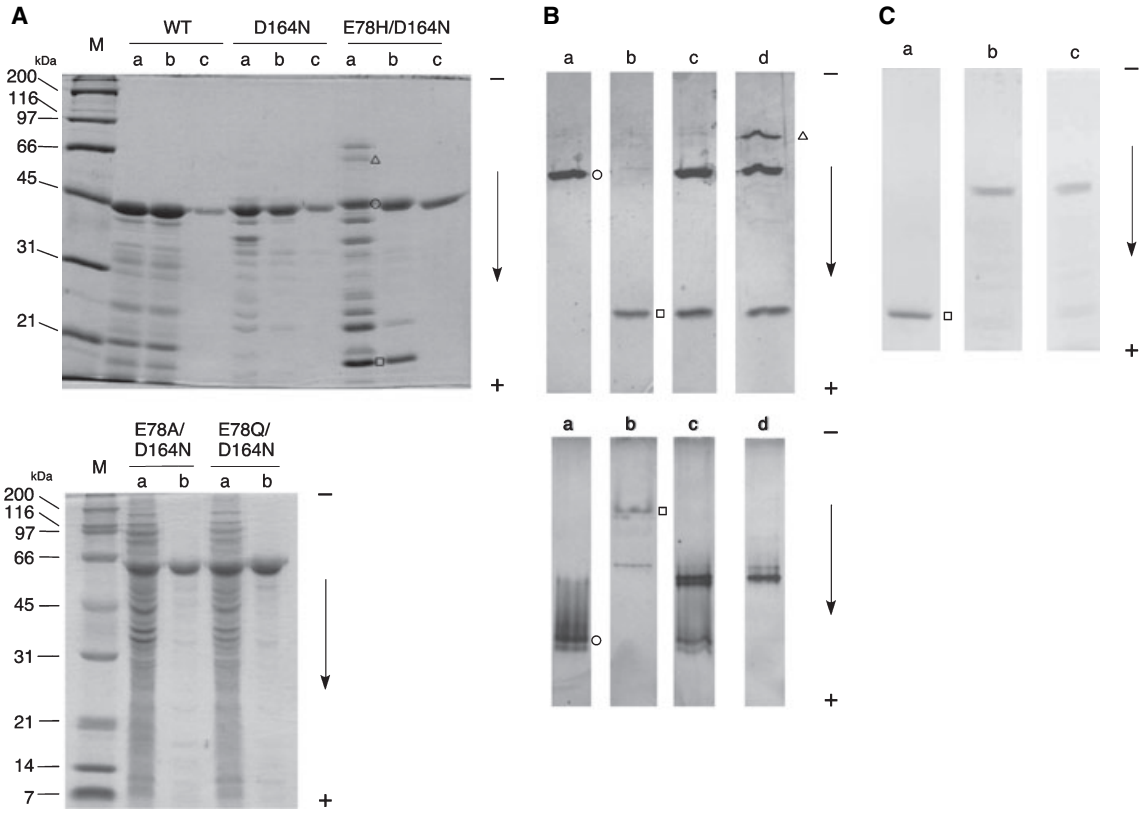

Fig. 2. PAGE analyses of the wild-type and mutants of kumamolisin-As. Arrows indicate the direction of electrophoresis. Open circles, open squares, and open triangles indicate the bands of the 38-kDa mature form, the 19-kDa propeptide, and the 57-kDa proenzyme of the E78H/D164N mutant, respectively. (A) SDS/PAGE of the wild-type (WT), D164N mutant (D164N), the E78H/D164N double mutant (E78H/D164N), the E78A/D164N double mutant (E78A/D164N), and the E78Q/D164N double mutant (E78Q/D164N). Lanes a, the crude extract of *E. coli* cells expressing the respective enzymes (4 μg each); lanes b, the supernatant solution obtained after the incubation of the crude extracts at pH 4.0 and 55 °C for 3 h (2 μg each); lanes c, purified mature forms of enzymes (0.3 μg each); lane M, marker proteins. Proteins were stained with Coomassie brilliant blue. The apparent molecular masses estimated on the basis of electrophoretic mobility of the mature forms and the proenzyme in SDS/PAGE were larger than the values calculated from the deduced amino-acid sequences. This arises from the anomalously low electrophoretic mobility of the enzyme in SDS/PAGE, which is probably due to the relatively high contents of acidic amino-acid residues in the enzyme [15]. (B) SDS/PAGE (upper panel) and nondenaturing PAGE (lower panel) analyses of the E78H/D164N mutant and related proteins. Lanes a, the purified 38-kDa mature form; lanes b, the isolated 19-kDa propeptide; lanes c, equimolar amounts of the purified 38-kDa mature form and the isolated 19-kDa propeptide are mixed; lanes d, the purified proenzyme (a mixture of the nicked and intact forms of the precursor). Proteins were detected by silver staining. The band of the 38-kDa mature form is smeared in nondenaturing PAGE (lower panel, lanes a and c). For details of purification of the 38-kDa mature form, 19-kDa propeptide, and proenzyme, see Experimental procedures. (C) The purified 19-kDa propeptide (lane a) was incubated with an equimolar amount of the 37-kDa mature form of the wild-type enzyme (lane c) at pH 4.0 and 50 °C for 10 min. The resulting mixture (lane b) was subjected to SDS/PAGE. Proteins were stained with Coomassie brilliant blue.

corresponded to that of the mature form and the N-terminal propeptide of the E78H/D164N mutant [15]. The 38-kDa protein could not be separated from the 19-kDa and 57-kDa proteins by anion-exchange chromatography at pH 7.0 but could only be isolated by hydroxyapatite chromatography at pH 4.3. The 19-kDa protein was isolated by ultrafiltration under denaturing conditions, followed by renaturation. When equimolar amounts of the isolated 38-kDa and 19-kDa proteins were mixed and subjected to nondenaturing PAGE, these proteins comigrated with each other, showing a broad protein band that differed from the respective original bands and almost coincided with the band of the 57-kDa precursor (Fig. 2B). These results strongly suggest that the mutant existed as a nicked precursor, with the scissile site being between His172p and Phe173p (Fig. 1), and the N-terminal 19-kDa fragment was noncovalently associated with the 38-kDa mature form. Unlike the E78H/D164N mutant, however, both the E78A/D164N and

E78Q/D164N mutants were completely inactive and existed as their 57-kDa precursor form even after heat treatment (Fig. 2A). In contrast, when equimolar amounts of the 19-kDa protein and the wild-type 37-kDa mature form were incubated at pH 4 and 50 °C for 10 min and then subjected to SDS/PAGE, the 19-kDa band disappeared, whereas the 37-kDa band remained (Fig. 2C).

During the course of our attempts to separate the 38-kDa mature form of the E78H/D164N mutant from the 19-kDa propeptide, we unexpectedly observed that incubation of the nicked form of the precursor at pH 7.0 at 4 °C resulted in a time-dependent enhancement of the 57-kDa band with a concomitant diminution of the 38-kDa and 19-kDa bands, as analyzed by SDS/PAGE (Fig. 3A). The 38-kDa and 19-kDa bands did not disappear completely after prolonged incubation (up to 24 h), and the ratio of band intensities of these three proteins eventually became constant. Automated Edman degradation of the 57-kDa species yielded a single amino-acid sequence, Ser-Asp-Met-Glu-Lys-, indicating that the 19-kDa protein was ligated to N-terminus of the 38-kDa protein. Moreover, when the resulting mixture was dialyzed overnight at 4 °C against 0.05 M sodium acetate buffer, pH 4.0, the 57-kDa band diminished whereas the 38-kDa and 19-kDa bands were enhanced (Fig. 3A, lane c). These observations suggest that, at pH 7.0, the 38-kDa and 19-kDa proteins can be reversibly ligated with each other to produce the full-length precursor and the ligation reaction was at equilibrium under the conditions. The rate of the formation of the full-length precursor was not enhanced when the nicked precursor was incubated at pH 7.0 and 4 °C with the 38-kDa

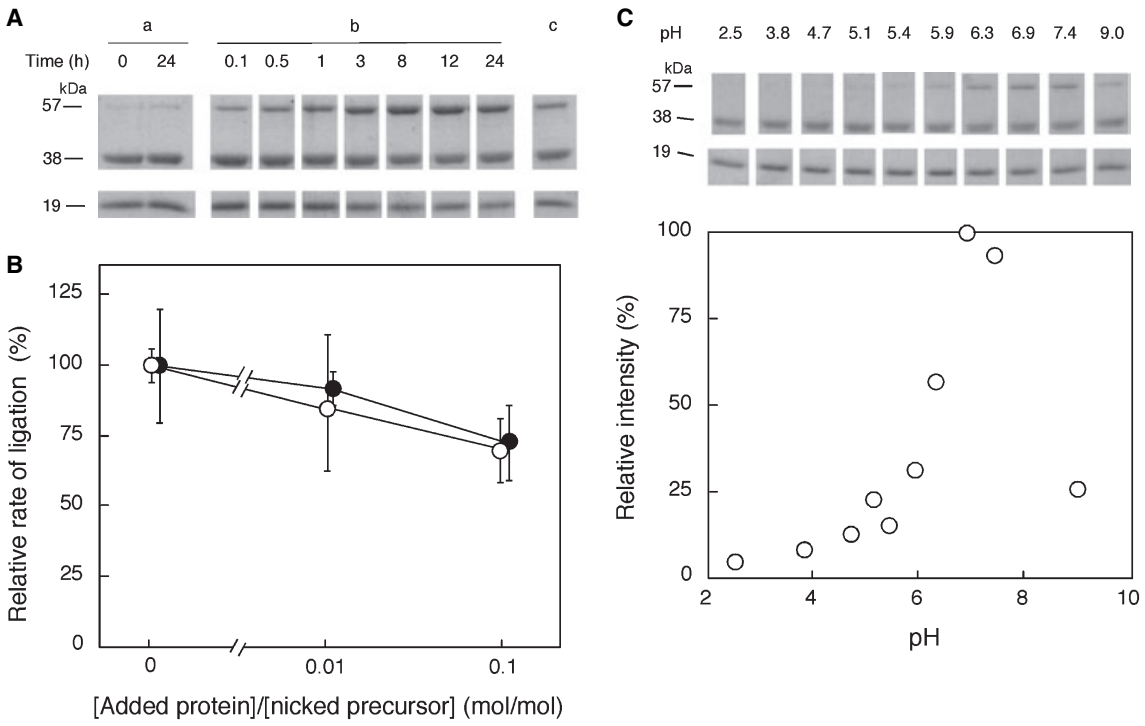

Fig. 3. SDS/PAGE analyses of ligation/cleavage process in the 57-kDa precursor of the E78H/D164N mutant. (A) The course of ligation in the nicked precursor and cleavage of the ligated product were analyzed as described in Experimental procedures. Lanes a, the nicked precursor in 50 mM sodium acetate buffer, pH 4.0 (left) was incubated in the same buffer at 4 °C for 24 h (right). Lanes b, the nicked precursor was incubated at pH 7.0 and 4 °C for indicated periods of time. Lane c, the nicked precursor was incubated at pH 7.0 and 4 °C for 24 h and then dialyzed overnight at 4 °C and pH 4.0. (B) Effects of addition of different amounts of the 38-kDa mature form (○) and the wild-type enzyme (●) on the rate of ligation. Catalytic and substoichiometric amounts (molar ratio of 0.01 and 0.1, respectively) of these proteins were incubated with the nicked precursor at pH 7.0 and 4 °C for 6 h, followed by SDS/PAGE. The rate of ligation was estimated from percentage intensity of the band of the 57-kDa protein in a total of intensities of the 57-kDa, 38-kDa and 19-kDa bands, where the intensity of the 38-kDa protein band was corrected for the amounts of the added proteins with similar sizes. The rates of ligation in the absence of added proteins were taken as 100%. The mean of the values of three independent experiments is shown with standard errors. (C) The pH-dependence of the ligation process. Upper panel shows SDS/PAGE analysis of the pH-dependence of the ligation process. For details, see Experimental procedures. Lower panel, the band intensities of the 57-kDa band in the upper panel were plotted against the incubation pH.

mature form of the E78H/D164N mutant (molar ratio 1 : 100–1 : 10) or the wild-type enzyme (molar ratio 1 : 100–1 : 10) (Fig. 3B). Incubation with the crude extract of *E. coli* cells (50 μg protein) also did not enhance the rate of formation of the full-length precursor (data not shown). These results strongly suggest that the ligation process does not arise from catalytic action of these additives, but takes place in an intramolecular manner between the noncovalent complex of the prosegment and mature enzyme. Formation of the full-length precursor was not observed when the acid-treated supernatant containing the expressed wild-type enzyme, D164N, or E78H was allowed to stand overnight at pH 7.0 and 4 °C (not shown).

The pH-dependence of the ligation process was examined over the pH range 2.5–9.0 at 4 °C by SDS/PAGE using the nicked precursor of the E78H/D164N mutant. Only a very low level of ligation took place at pH 2.5–4.7, so that the mutant precursor stably existed as its nicked form under acidic conditions. At pH above 5.1, the rate of ligation was higher, increasing with pH until it became constant at pH 6.9–7.4 (Fig. 3C). At pH 9.0, the rate of ligation was lower than that at pH 7.4, probably because of the instability of the enzyme under alkaline conditions (see Experimental procedures).

The active site

The 37-kDa and 38-kDa mature forms of D164N and E78H/D164N, respectively, were subjected to X-ray crystallographic studies. Crystals of the D164N mutant of kumamolisin-As were fully isomorphous with those of the uninhibited wild-type enzyme and of the E78H mutant, and the structures are very similar (r.m.s.d. 0.264 and 0.312 Å for 350 Cα pairs). Crystals of the E78H/D164N mutant are completely different and contain two independent molecules in the asymmetric unit. These two molecules can be superimposed, with r.m.s.d. 0.15 Å for 338 Cα pairs; arbitrarily, molecule A (Fig. 4A) is used for the comparisons described here. This difference in crystal types makes it possible to separate the influence of lattice forces from the mutation effects.

The electron density corresponding to the active site is excellent in all structures (Fig. 4B). The conformation of His78 is virtually identical in the single and double mutants involving this residue (Fig. 5B,D). In both cases, the side chain is removed from the vicinity of Ser278 and Asp82 and the catalytic triad does not exist in the observed structures. The position of His78 is stabilized by a short hydrogen bond with the Oγ of Ser128; that atom is, in turn, also hydrogen-bonded to Oδ1 of Asp82. Surprisingly, the catalytic Ser278 makes direct hydrogen bonds with the side chain group of Asn164 in both the D164N and E78H/D164N mutants of kumamolisin-As (Fig. 5C,D). The distance between the parent atoms is 2.82 Å in the D164N mutant and 3.34 Å in the E78H/D164N mutant, with the torsion angles of the residues being virtually identical. This is in contrast with a water-mediated interaction between the serine and the carboxy group of Asp164, observed

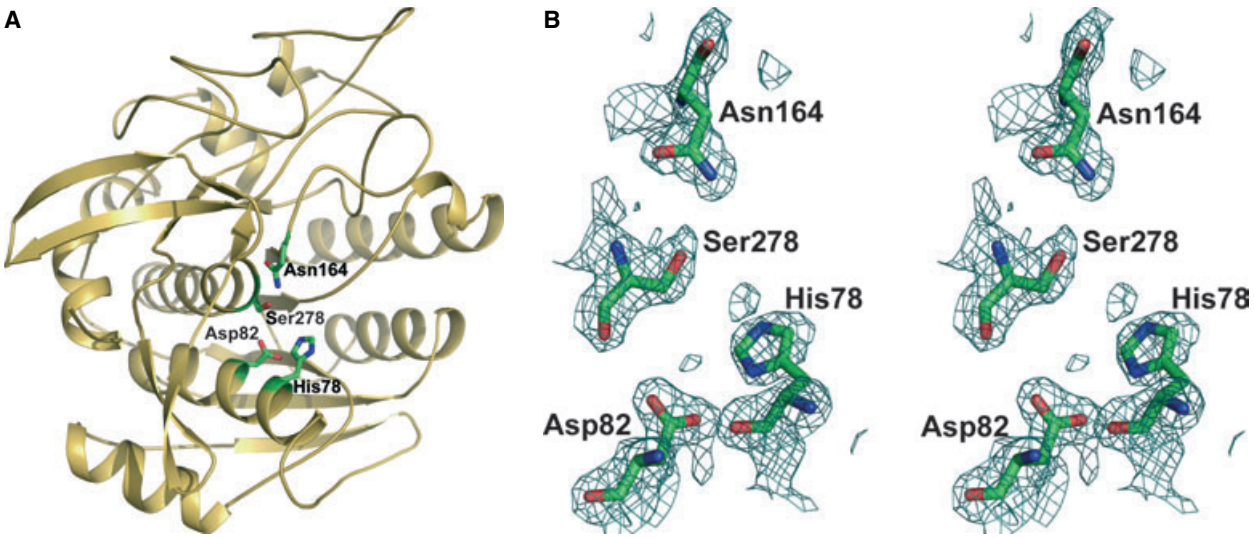

Fig. 4. The structure of kumamolisin-As and its active site. (A) Backbone tracing of the E78H/D164 double mutant, with the active-site residues shown by stick representation. (B) $2F_o$-F_c omitmap electron density calculated with phases obtained from a model from which the active-site residues were removed, contoured at 1σ level.

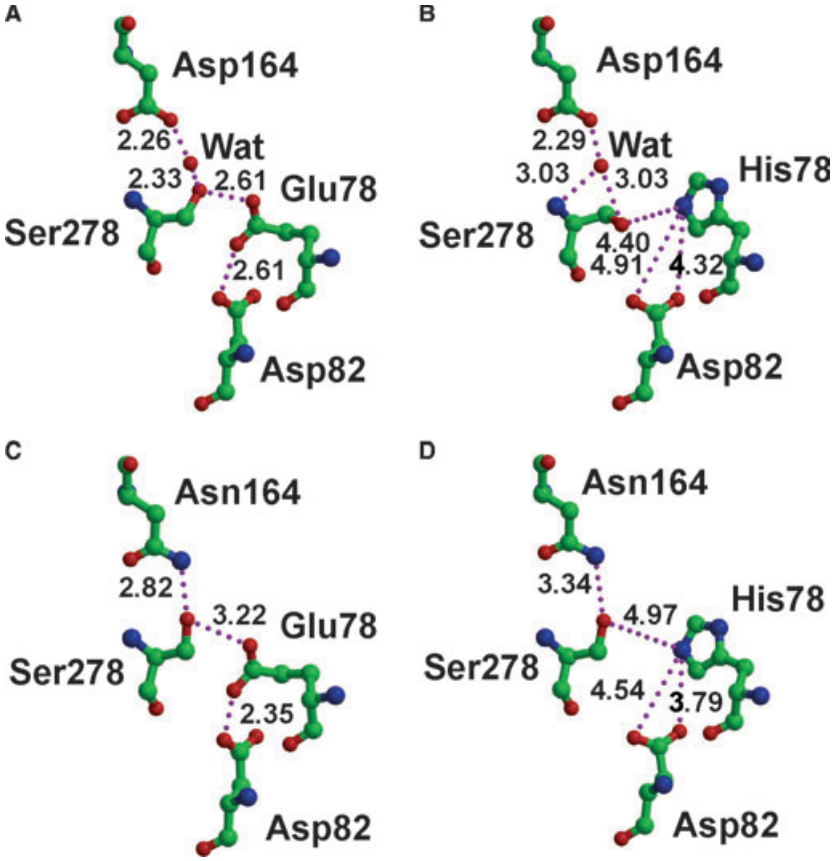

Fig. 5. Close-up view of active sites, with marked distances between hydrogen-bonded groups. (A) Uninhibited wild-type kumamolisin-As; (B) E78H mutant; (C) D164N mutant; (D) E78H/D164 double mutant.

in both the wild-type and E78H enzyme (Fig. 5A,B). Although it is not possible to distinguish between the Oδ1 and Nδ2 of Asn164 directly, analysis of the hydrogen-bonded networks indicates that the latter atom serves as a hydrogen-bond donor and Ser278 is an acceptor.

In the structures of the wild-type kumamolisin-As and two of its mutants, the conformation of the catalytic Ser278 is quite similar, with the side chain torsion angle χ1 of −78 ° in the wild-type enzyme, −33 ° in D164N, and −41 ° in the E78H/D164N mutant. In contrast, this torsion angle is 74 ° in the structure of the E78H mutant, and, in that case, the Oγ atom of Ser278 interacts only with two water molecules. One of them is a highly conserved water (Wat570) which is also bound to the main chain carbonyl of Gly275, and the other is Wat648, which mediates an interaction with the carboxylate group of Asp164 (Fig. 5B). Wat786, an equivalent of Wat648 found in the wild-type structure, has a considerably higher temperature factor, yet it also mediates the interactions between Ser278 and Asp164. Thus the introduction of an asparagine instead of an aspartic acid into the oxyanion hole had the unexpected result of shifting the side chain of residue 164 closer to the catalytic serine and eliminating the water molecule that mediated their contact in the wild-type enzyme. It is clear that this interaction is not influenced by whether residue 78 is a Glu or a His, as both the D164N and E78H/D164N mutants make similar interactions.

pH-dependent kinetic studies

Kinetic parameters of the mature forms of D164N and E78H/D164N for hydrolysis of the internally quenched fluorogenic (IQF) substrate, NMA-MGPH*FFPK-(DNP)DRDR {[2-(*N*-methylamino) benzoyl]-L-methionyl-glycyl-L-prolyl-L-histidyl-L-phenylalanyl-L-phenylalanyl-L-prolyl-(N^{ε}-2,4-dinitrophenyl)-L-lysyl-D-arginyl-D-arginine amide}, were determined at pH 4.0 and 40 °C, and the results are compared in Table 1 with the previously reported values obtained for the wild-type enzyme and for the E78H mutant. As observed with the E78H substitution, both the single D164N and the E78H/D164N double substitutions caused significant loss of enzyme activity (k_{cat} 1.3% and 0.0001% of that of the wild-type enzyme, respectively).

Table 1. Kinetic parameters of kumamolisin-As mutants. Parameters are those for enzymatic hydrolysis of NMA-MGPH*FFPK-(DNP)DRDR catalyzed by mature forms of the respective enzymes at pH 4.0 and 40 °C. Values in parentheses indicate relative percentage of k_{cat} and k_{cat}/K_m values of mutants, with those of wild-type enzyme taken to be 100%. For E78H/D164N, a mixture of the nicked and intact forms of the precursor could also be obtained (see Results section), but was unable to process the IQF substrate.

Mutant	k_{cat} (s^{-1})	K_m (μM)	k_{cat}/K_m ($s^{-1}\cdot\mu M^{-1}$)
Wild-type[a]	395 ± 7 (100)	1.0 ± 0.2	395 (100)
E78H[a]	0.033 ± 0.006 (0.008)	0.7 ± 0.2	0.047 (0.012)
D164N	5.3 ± 0.2 (1.3)	0.8 ± 0.1	6.6 (1.7)
E78H/D164N	0.00045 ± 0.00005 (0.0001)	nd[b]	nd[b]

[a]Values are quoted from [7]. [b]K_m values could not be determined because, owing to the extremely low catalytic activity, the assay of this mutant required high concentration of the mutant (e.g. 150 nM), which was not significantly lower than the substrate concentration used in the kinetic studies.

The kinetic parameters for the wild-type enzyme, E78H, D164N, and E78H/D164N were also determined over the pH range 2.5–8.0 (Fig. 6), at which enzyme stability is maintained under the assay conditions. For the wild-type enzyme, the pH-dependence of the $\log(k_{cat}/K_m)$ value showed a bell-shaped profile with apparent pK_a values of 3.8 and 5.8, whereas the $\log k_{cat}$ vs. pH profile displayed a profile with slope = −1 which leveled off at low pH values with an apparent pK_a of 5.9 (Fig. 6A). The k_{cat}/K_m and k_{cat} values of E78H were essentially independent of pH in the pH range used here (Fig. 6B). The $\log k_{cat}$ vs. pH and $\log(k_{cat}/K_m)$ vs. pH profiles of D164N were similar to those of the wild-type enzyme, although a shift in an apparent pK_a to 6.6 was observed in the $\log(k_{cat}/K_m)$ vs. pH profile (Fig. 6C). In contrast, the $\log k_{cat}$ vs. pH of E78H/D164N displayed a sigmoidal profile with an apparent pK_a of 7.0 (Fig. 6D), which is reminiscent of that of subtilisin. [It is highly unlikely that the observed very weak peptidase activity of the purified E78H/D164N mutant arose from contamination by activities of *E. coli* proteinases, because the control experiment showed the absence of any proteinase activity in the supernatant of the acid-treated crude extract of *E. coli* cells harboring the plasmid without an inserted DNA (see Experimental procedures). The observed intramolecular ligation/cleavage process of the E78H/D164N precursor also corroborates the very weak activity of the mutant (see Discussion).] However, the double mutant was unable to act on benzyloxycarbonyl-L-alanyl-L-alanyl-L-leucine *p*-nitroanilide, a substrate that has often been used for subtilisin assays [16].

Discussion

Mutants of kumamolisin-As were created in order to change the pH optimum of this enzyme and to evaluate the reasons for the similarity and differences in its mechanism compared with subtilisin. A residue in the putative oxyanion hole (Asp164) and one of the residues in the catalytic triad (Glu78) were mutated singly and as a pair. It must be stressed that we did not aim to create a truly subtilisin-like active site, as Asp82, the residue of the triad that is conserved in its nature but is topologically different in these two classes of peptidases, was not mutated. X-ray crystallographic analyses of these mutants, D164N and E78H/D164N, revealed that they have altered hydrogen-bond networks in their active site. Consistent with these observations, both mutants exhibited low enzymatic activities. However, the fate of the N-terminal propeptide produced after processing and the pH-dependent kinetic behavior were different for different mutants.

Despite the fact that the purified 38-kDa mature form of the E78H/D164N mutant showed only very low activity (k_{cat} 0.00045 s^{-1} at pH 4.0 and 40 °C), the observed processing of the mutant can consistently be explained in terms of intramolecular (unimolecular) cleavage of the precursor, in which a molecule of the mutant cleaves its own propeptide, as proposed for some sedolisins including kumamolisin [12,13]. The intramolecular cleavage is completed as a single turnover process, and the E78H/D164N mutant is estimated to be capable of operating once per ≈2200 s (≈ 37 min) (at pH 4 and 40 °C), hence, the present conditions of bacterial cultivation through enzyme purification are sufficient for this cleavage to take place. These considerations also corroborate the observed instantaneous transformation of precursors of the wild-type and D164N mutant into their 37-kDa forms. It is likely that the N-terminal propeptide functions as an intramolecular chaperone to facilitate the correct folding of the nascent polypeptide chain of the precursor [3,13]. For the wild-type enzyme and the D164N mutant, the full-length precursor, once correctly folded, instantaneously cleaves the peptide bond between His172p and Phe173p by themselves. The resulting 19-kDa fragment must be released from the mature form and immediately degraded through multiple attack by the mature form, judging from the fact that the incubation of the 19-kDa propeptide with the wild-type enzyme at pH 4 and 50 °C (growth conditions of the strain NTAP-1, the kumamolisin-As-producing bacterium) resulted in immediate degradation of the propeptide (see Results). As the mature form of the wild-type enzyme is found to start with Ala1e [15]

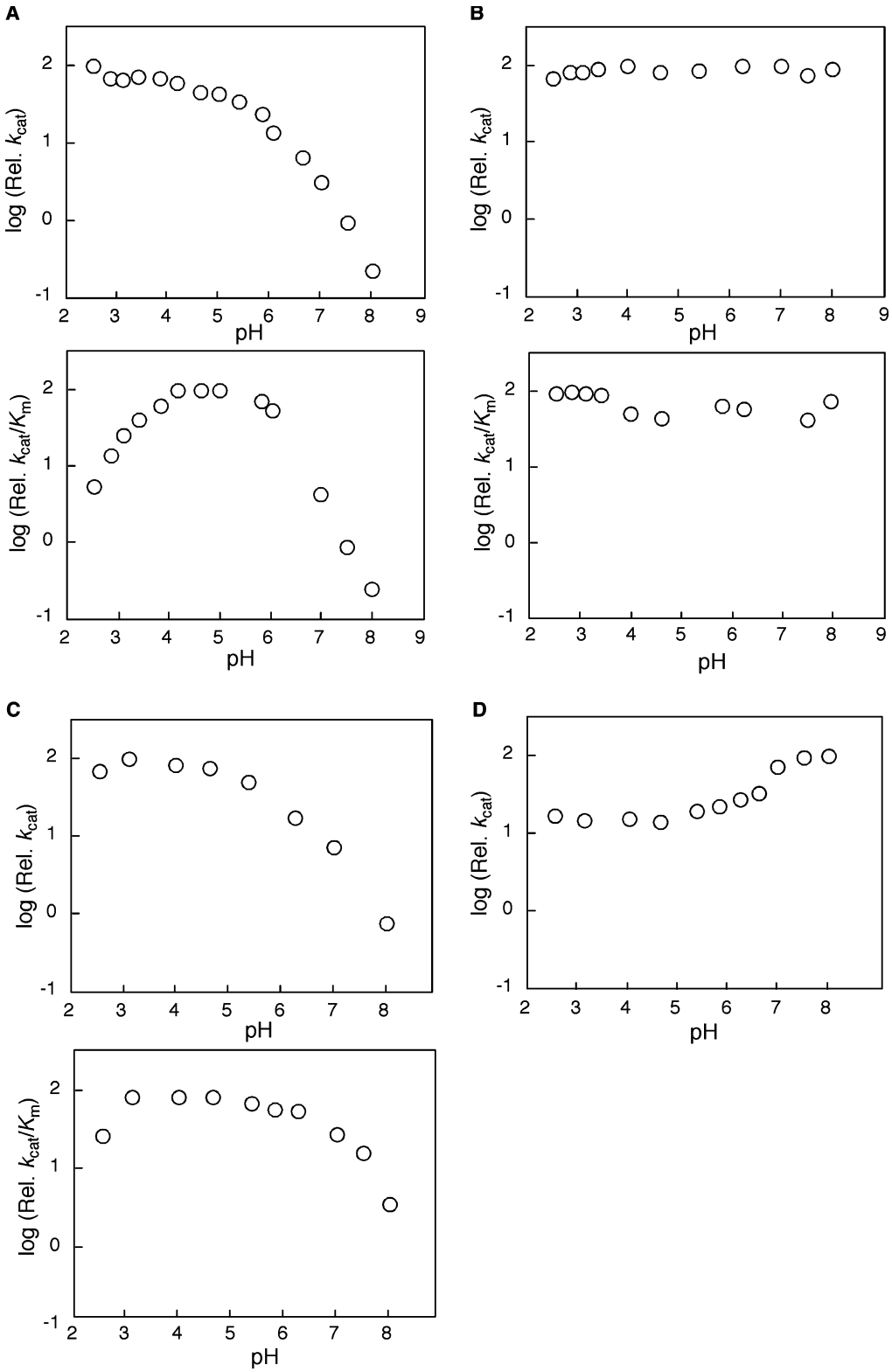

Fig. 6. Effects of pH on log(relative k_{cat}) (upper panels) and log(relative k_{cat}/K_m) (lower panels) of hydrolysis of NMA-MGPH*FFPK-(DNP)DRDR by wild-type kumamolisin-As (A), E78H (B), D164N (C), and E78H/D164N (D). Standard errors of kinetic data were within ± 20%. The experimental conditions were as described in Experimental procedures.

(or with Thr4e [7]), the linker part (Fig. 1) must be further truncated, probably by *E. coli* peptidases [13]. In contrast, because of its very low catalytic activity, the E78H/D164N mutant cannot degrade the 19-kDa propeptide, which remained noncovalently associated with the mature form. These analyses suggest that, in the intracellular milieu (pH $\approx$ 7) of *E. coli*, the expressed E78H/D164N mutant exists as an equilibrated mixture of the nicked and intact forms of the precursor, alternating ligation and cleavage in an intramolecular manner. It is also plausible that the nicked form of the precursor escapes truncation of the linker part by the *E. coli* proteinases.

Previous structural and mutagenesis studies of kumamolisin, which is 93% identical with kumamolisin-As in its primary structure, showed that substitution of Asp164 by Ala abolished the catalytic activity of the enzyme, which was thus unable to be autoactivated and remained as its 57-kDa precursor [6]. This, along with the fact that Asp164 is located at the oxyanion hole, suggested that Asp164 is involved in stabilization of the transition-state oxyanions that develop during catalysis [7]. Moreover, recent computational studies of kumamolisin-As catalysis using quantum mechanical/molecular mechanical molecular dynamics simulations predicted that, in the wild-type enzyme, the transition-state oxyanions are stabilized by proton transfer from Asp164, which thus acts as a general acid/base catalyst [17]. Therefore, this enzyme may utilize a strategy of aspartic peptidase catalysis, in addition to that of serine peptidase catalysis. Unlike the case of Asp164Ala substitution in kumamolisin, a low but appreciable level of catalytic activity was found with the purified D164N mutant of kumamolisin-As. Structural analyses of the mutant showed that the hydrogen bonds between Ser278 and Glu78 and those between Glu78 and Asp82 exist, although the mutated residue unexpectedly makes a hydrogen bond with the side chain of Ser278. The presence of some relatively short hydrogen bonds does not appear to be an artifact of refinement, as indicated by the generally high quality of the electron-density maps. These results suggest that this perturbed catalytic machinery, with an amide side chain at the oxyanion-binding site, are, at least in part, capable of mediating peptidase catalysis, although it did not operate in exactly the same way as in the wild-type enzyme. The side chain of Asn164 of D164N must be unable to fulfill the general acid/base role; however, it might be able to stabilize the transition states in an alternative manner, i.e. through polar interactions, as in the case of Asn155 of subtilisins. It should be noted that the IQF substrate used in the present enzyme assays possesses a histidine at its P1 position, raising an alternative possibility that the D164N mutant itself might be inherently inactive, and the observed low catalytic activity of the mutant might arise from substrate-assisted catalysis [18], where a His at P1 from the substrate might interact directly with the oxygen atom of the scissile peptide bond to act as the general acid catalyst. However, this appears to be unlikely, judging from the fact that the D164A mutant of kumamolisin remains an inactive 57-kDa precursor, with His172p located at P1 and unable to assist autocatalytic activation [6]. The pH-dependences of k_{cat} and k_{cat}/K_m values were similar to those of the corresponding values of the wild-type enzyme. This observation should not necessarily mean that Asp164 is unimportant in the preference of the catalytic activity for acidic pH because this mutant retains other candidates that may be responsible for the preference of the enzyme activity for acidic pH (e.g. Glu78). The involvement of the β-amide hydrogen of the Asn164 residue in the catalysis of D164N as well as the importance of Asp164 for the low-pH peptidase activity are also implicated from a comparison of the kinetic results obtained with E78H and E78H/D164N (see below).

The 38-kDa mature form of the E78H/D164N mutant was separated from the 19-kDa propeptide by hydroxyapatite chromatography at pH 4.3. The His78 of the mutant is removed from the vicinity of Ser278 and Asp82 and the catalytic triad does not exist. The catalytic triad was also absent in the crystal structure of the single E78H mutant [7]. In both of these mutants, it is possible to create a strong hydrogen bond between Ser278 and His78 by changing only the torsion angles of the side chains (without adjustment of any main-chain parameters), but it is not possible to adjust His78 in any way that would result in that residue also making a hydrogen bond with Asp82. As previously proposed for sedolisin [19] and for kumamolisin [6], the side chain of Glu78 of the wild-type enzyme should be protonated at pH 3–4. Thus, the His78 residues of E78H and E78H/D164N are likely to be protonated because the intrinsic pK_a of the imidazole group (6.0) of histidine is higher than that of the γ-carboxyl group (4.2) of glutamic acid. This should at least in part explain why a hydrogen bond between His78 and Ser278 cannot be created in these mutants at pH 4. Thus, the very low catalytic activities of E78H and E78H/D164N must be due to the inability of Ser278 to be activated at acidic pH. Importantly, however, the E78H/D164N mutant showed a small increase in its peptidase activity at neutral pH. The k_{cat} values at neutral pH were 7–8 times higher than the values at acidic pH, displaying an apparent pK_a of

≈ 7.0, which is reminiscent of the pH–activity profiles of subtilisins and other classical serine peptidases. This profile was distinct from those of the wild-type and any other catalytically active mutants of kumamolisin-As. Moreover, the fact that both the E78A/D164N and E78Q/D164N mutants were completely inactive indicates that the observed shift of the pH optimum did not reflect general effects of amino-acid substitutions, but specifically arose from the E78H/D164N double substitution. To the best of our knowledge, this is the first example of the conversion of a peptidase active at low pH to a peptidase active at neutral pH. However, it is highly unlikely that the increase in activity at neutral pH is mediated by the Ser278-His78-Asp82 triad in the mutant, judging from the fact that no hydrogen bond between His78 and Asp82 was created. More likely, this pH–activity profile arose from catalysis mediated by a Ser278-His78 dyad at neutral pH. The imidazolium group of His78 must be deprotonated at neutral pH to make a hydrogen bond with the side chain of Ser278 and act as a weak general base catalyst (without the help of Asp82), making an inefficient surrogate of the γ-carboxy group of Glu78 of the wild-type enzyme. Moreover, a comparison of log k_{cat} vs. pH profiles of the E78H and E78H/D164N mutants provides clues to understanding the importance of peptidase catalysis of a hydrogen-donating group(s) located at the oxyanion hole [9,10]. Unlike for the E78H/D164N mutant, the k_{cat} value of the single E78H mutant did not show any enhancement at neutral pH values, probably because the side chain of Asp164 of E78H would be in its carboxylate ($-COO^-$) form at neutral pH and unable to stabilize the oxyanion that develops during cleavage of the peptide bond. In contrast, the γ-amide hydrogen of the Asn164 residue of E78H/D164N may participate in stabilization of the transition state, irrespective of the pH, so that the E78H/D164N mutant showed a small increase in its peptidase activity at neutral pH. In addition, the observed dramatic switch of pH-dependence of the k_{cat} value upon the E78H/D164N substitution suggests that the observed pK_a value (5.9) of k_{cat} of the wild-type must arise from titration of Glu78 and/or Asp164. Elevated pK_a values of these residues have been predicted by Bode's group on the basis of clustering of many acidic residues around these two residues [6].

The observed ligation/cleavage of the E78H/D164N precursor was a reversible, pH-dependent, unimolecular process, the pH profile of which resembles that of the k_{cat} vs. pH profile of the mutant. Cleavage of the precursor did not take place when His78 of this precursor molecule was replaced by either alanine or glutamine. Thus, this process appears to be consistently described in terms of the dyad-mediated mechanism mentioned above (Fig. 7). With the nicked form of the precursor as the starting species (Fig. 7, step 1), His78, which favors its deprotonated form at neutral pH, activates Ser278 to facilitate its nucleophilic attack on the carbonyl carbon of the C-terminal carboxy group of the associated 19-kDa propeptide, producing an oxyanion. The His78 subsequently abstracts a proton from the

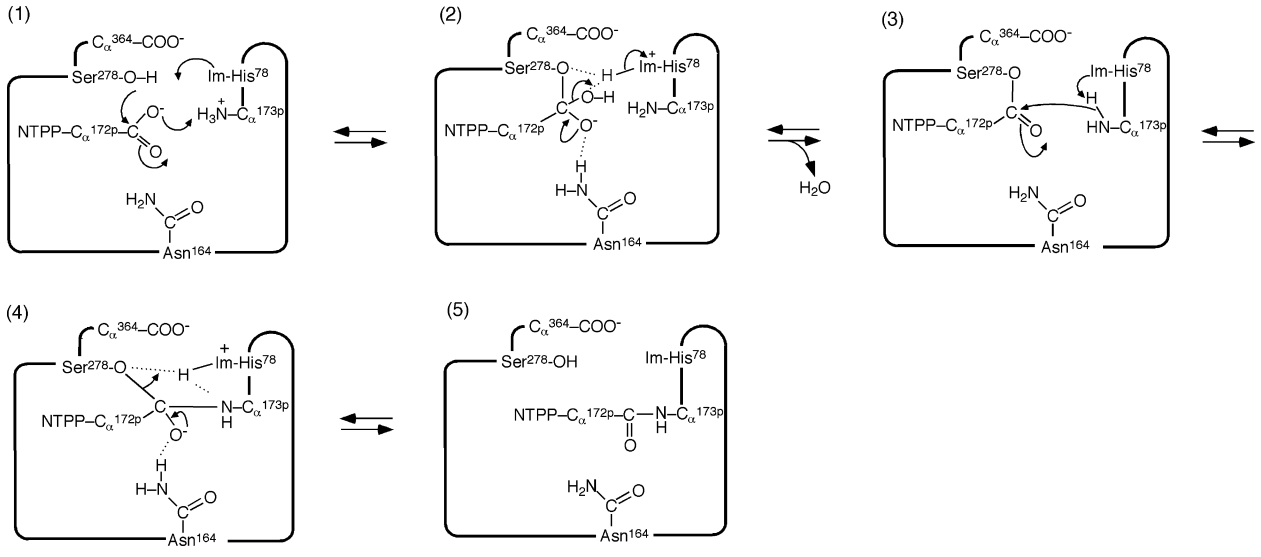

Fig. 7. Proposed mechanism of the ligation/cleavage process mediated by the His78-Ser278 dyad as well as Asn164 of the E78H/D164N mutant precursor. Thick lines indicate the polypeptide chain of the 38-kDa mature form of the mutant. C_α^{172p}, C_α^{173p}, and C_α^{364} denote α carbons of His172p, Phe173p, and Pro364, respectively, and Im denotes the imidazole group of His78. NTPP, N-Terminal propeptide.

N-terminal amino group of its own polypeptide (the 38-kDa mature protein), facilitating formation of the C–N linkage between His172p and Phe173p. The side chain of Asn164 must play an important role in stabilizing the transition-state oxyanions. With the intact form of the precursor as the starting species (Fig. 7, step 5), the reverse of this process would take place, which corresponds to the single turnover process of the mechanism proposed for the peptidase activity at neutral pH as described above. The ratio of amounts of the nicked vs. intact species would be determined by the equilibrium of these forward and reverse reactions.

At acidic pH, the mutant protein must be in a different protonation state, resulting in a shift of the equilibrium to that favoring cleavage. Although the mechanistic details of the cleavage at acidic pH remain to be clarified, a plausible mechanism is that the protonated His78 acts as a general acid which donates a proton to the amide nitrogen of the peptide to destabilize the amide bond. The resulting deprotonated form of His78 activates Ser278 to facilitate its nucleophilic attack on the carbonyl carbon, producing an oxyanion, followed by amide bond cleavage. This single turnover process could be extended to multiple turnover processes, which might account for the observed very weak peptidase activity of the E78H/D164N mutant at pH 3–5 (Table 1 and Fig. 6D). The reverse process must be unfavorable because the protonated His78 cannot induce the nucleophilic attack by Ser278 that triggers peptide bond formation.

In conclusion, the observed switch of the pH-dependent kinetic behavior upon the E78H/D164N double substitutions as well as the observed ligation/cleavage equilibrium of the resulting precursor corroborate the mechanistic importance of the glutamate-mediated catalytic triad and aspartic acid residue located at the oxyanion hole that has been proposed from structural studies of sedolisins for the preference of their catalytic activity for acidic pH [4,5]. The grafted Asp-His-Ser triad and oxyanion-stabilizing Asn residue were found to function only incompletely, probably because this canonical catalytic machinery could not fully be adapted in the sedolisin scaffold. We are currently undertaking additional studies in an attempt to obtain a suppressor mutant of E78H/D164N that exhibits higher neutral peptidase activity.

Experimental procedures

Materials

The IQF substrate, NMA-MGPH*FFPK-(DNP)DRDR, and benzyloxycarbonyl-L-alanyl-L-alanyl-L-leucine *p*-nitroanilide [16] were products of the Peptide Institute, Osaka, Japan. An inhibitor, AcIPF (*N*-acetyl-isoleucyl-prolyl-phenylalaninal), was synthesized as described previously [19,20]. Restriction enzymes and other DNA-modifying enzymes were purchased from TaKaRa Shuzo, Kyoto, Japan or from Toyobo, Osaka, Japan. The plasmid pScpA, which is a derivative of pET15b (Novagen, Madison, WI, USA), was constructed as described previously [15] and was used for the expression of the wild-type kumamolisin-As gene. All other chemicals used were of analytical or sequencing grade, as appropriate.

Mutagenesis, protein expression, and protein purification

Construction of the plasmid pScpA/E78H expressing the active-site mutant E78H, in which glutamic acid was replaced by a histidine, was as previously described [7,15]. The plasmids, pScpA/E78H/D164N and pScpA/D164N, expressing the E78H/D164N and D164N mutants, were constructed by *in vitro* mutagenesis of the plasmid pScpA/E78H (for pScpA/E78H/D164N) and pScpA, respectively, using a QuickChange Mutagenesis Kit (Stratagene, La Jolla, CA, USA) according to the manufacturer's guidelines. Additional plasmids, pScpA/E78A/D164N and pScpA/E78Q/D164N, which expressed the E78A/D164N mutant and the E78Q/D164N mutant, respectively, were created by PCR-based mutagenesis on pScpA/D164N. Individual mutations were verified by DNA sequencing on both strands using a Dye-terminator Cycle Sequencing Kit (Beckman Coulter, Fullerton, CA, USA) with a CEQ 2000 DNA analysis system (Beckman Coulter). Expression of wild-type and mutated kumamolisin-As was carried out essentially as described previously [15]. Purification of the expressed product was completed at 0–5 °C, unless otherwise stated. To avoid possible contamination of mutant preparations with the wild-type enzyme activity during purification, purification of the mutants was completed first, followed by that of the wild-type enzyme. Moreover, centrifugal ultrafiltration devices, microtubes, and test tubes used during enzyme purification were discarded after a single use. The wild-type enzyme was purified to homogeneity as described previously [7]. The D164N mutant (the 37-kDa mature form) and the E78H/D164N mutant (a mixture of the nicked and intact forms of the precursor, see the Results section) were purified to homogeneity essentially as described for the wild-type enzyme, except that a MonoQ HR10/10 column [7] was replaced by disposable HiTrapQ columns (5 mL; Amersham Biosciences, Piscataway, NJ, USA) and a single HiTrapQ column was exclusively used for purification of each mutant. For purification of the 38-kDa mature form of the E78H/D164N mutant, the crude extract of the *E. coli* transformant cells (prepared with 0.05 M sodium acetate buffer, pH 4.0) was incubated at 55 °C for 3 h. After

centrifugation, the supernatant was dialyzed at 4 °C overnight against 5 mM KH_2PO_4/acetate buffer, pH 4.3. The protein solution was subjected to fast protein liquid chromatography on a Macro-Prep Ceramic Hydroxyapatite (Type I; particle size, 40 μm; Bio-Rad) column (10 × 100 mm) that had previously been equilibrated with 5 mM KH_2PO_4/acetate buffer, pH 4.3. After extensive washing of the column with the equilibration buffer, the 38-kDa mature form of the mutant was eluted with a linear gradient of 5–360 mM KH_2PO_4 in 45 min at a flow rate of 1.0 mL·min^{-1}. During purification, the mutant protein was identified by SDS/PAGE [21] and further confirmed by analyzing the N-terminal amino-acid sequence [15] by automated Edman degradation after electroblotting of protein bands in SDS/polyacrylamide gels to nitrocellulose membranes. Nondenaturing PAGE was performed with a 7% gel by the procedure of Davis [22]. SDS/PAGE was carried out with a 10% gel by the method of Laemmli [21].

It should be noted that the acid treatment (at pH 4.0 and 55 °C for 3 h) of the crude extract of *E. coli* cells completely eliminated endogenous peptidases active at acidic pH. This was confirmed as follows. The crude extract of the *E. coli* BL21(DE3) host cells harboring pET15b (without an inserted DNA) was acid-treated as described above, followed by centrifugation, by which almost all of the *E. coli* proteins were removed as a precipitate. The supernatant was dialyzed at 4 °C overnight against 50 mM potassium phosphate buffer, pH 8.0, or 50 mM sodium acetate buffer, pH 4.0. Incubation of the resulting solutions with the IQF substrate, NMA-MGPH*FFPK-(DNP)DRDR (final concentration, 20 μM) at 40 °C for 1 h caused no detectable increase in fluorescence intensity.

Isolation of the 19-kDa propeptide of the E78H/D164N mutant

To study the binding and ligation of the 19-kDa propeptide to the 38-kDa mature form of E78H/D164N (see the Results section and Fig. 2B), we established a convenient procedure for obtaining the homogeneous 19-kDa propeptide from the crude extract of the *E. coli* transformant cells producing the E78H/D164N precursor. The crude extract (prepared with 50 mM sodium acetate buffer, pH 4.0) was incubated at 55 °C for 3 h. After centrifugation, the supernatant was concentrated by ultrafiltration with an Amicon Ultra device (Millipore, Bedford, MA, USA) (10 kDa molecular mass cut-off). The concentrate (100 μL) was mixed with 900 μL 50 mM sodium acetate buffer, pH 4.0, containing 8 M urea and allowed to stand overnight at room temperature. The resulting solution was then subjected to ultrafiltration with an Amicon Ultra device (30 kDa molecular mass cut-off). The filtrate, which contained homogeneous 19-kDa propeptide, was dialyzed against 50 mM sodium acetate buffer, pH 4.0. The 19-kDa propeptide could be quantitatively recovered as its soluble, renatured form.

Crystallization

Crystals of uninhibited kumamolisin-As mutants D164N and E78H/D164N were prepared as described previously [7]. Crystallization buffer contained 0.2 M ammonium sulfate and 30% PEG8000 in deionized water, at pH 4.6. Triclinic D164N crystals were isomorphous with the previously described crystals of the wild-type uninhibited kumamolisin-As and its E78H mutant and contained a single molecule in the asymmetric unit. The E78H/D164N mutant crystallized in monoclinic space group $P2_1$ with two molecules in the asymmetric unit, in a crystal form not described previously for this enzyme.

X-ray crystallographic data collection and structure refinement

Crystals were transferred to a cryogenic buffer containing 5% ethylene glycol, 0.2 M ammonium sulfate, and 30% PEG8000. X-ray diffraction data were collected at 100 K on a MAR345 detector mounted on a Rigaku H3R rotating anode X-ray generator, operated at 50 kV and 100 mA. The reflections were integrated and merged using the HKL2000 suite [23], with the results summarized in Table 2. Data for the D164N mutant were refined directly using the wild-type co-ordinates (PDB accession code 1SN7) to initiate the process. The structure of the E78H/D164N mutant was solved by molecular replacement with the program AMoRe [24], with the 2.3 Å structure of the E78H mutant [7] used as a search model. Two monomers of the E78H/D164N mutant were located in an asymmetric unit with a correlation coefficient of 0.619 and *R* factor of 37.1%. The structures were refined using the program SHELXL [25], by procedures similar to those used for the wild-type and E78H enzymes [7]. After each round of refinement, the models were compared with the respective electron-density maps and modified using the interactive graphics display program O [26]. The default shelxl restraints were used for the geometrical [27] and displacement parameters; temperature factors were refined isotropically, because of the limited resolution of data. Water oxygen atoms were refined with unit occupancies, although some of the sites are probably only partially occupied. The refinement results are also presented in Table 2. The co-ordinates and structure factors have been deposited in the Protein Data Bank (accession codes 1ZVJ and 1ZVK for the D164N and E78H/D164N mutants, respectively). For comparisons, the structures were superimposed with the program ALIGN [28].

Enzyme assay

Kinetic parameters for the enzymatic hydrolysis of the IQF substrate were determined as described previously [7]. The standard assay mixture contained various amounts of the

Table 2. Details of X-ray crystallographic data collection and structure refinement.

Crystal	D164N	E78H/D164N
Space group	*P*1	$P2_1$
Unit cell dimensions (Å)		
a	41.85	58.05
b	44.66	74.81
c	49.07	78.38
α	114.9	90
β	105.9	103.08
γ	102.1	90
Resolution (Å)	2.02	2.04
Measured reflections	36567	145143
R_{merge} (%)	4.4 (14.3)[a]	8.4 (21.0)
$I/\sigma(I)$	20.3 (5.5)	14.9 (4.7)
Completeness (%)	92.7 (76.1)	97.9 (79.2)
Refinement:		
R- no σ cutoff (%)	18.4	18.8
R_{free} (%)	26.3	29.2
Refl. used in refinement	16469	38838
Refl. used for R_{free}	870	607
Rms bond lengths (Å)	0.005	0.009
Rms angle distances (Å)	0.019	0.029
Protein atoms	2527	5056
Ligand atoms[b]	6	2
Water sites	240	444
PDB accession code	1ZVJ	1ZVK

[a]Values in the highest resolution shell are shown in parentheses. [b]One Ca^{2+} ion is present in all molecules; one sulfate ion is bound to the enzyme molecule in the D164N structure.

substrate, 50 mM sodium acetate buffer, pH 4.0, and the enzyme in a final volume of 300 μL. The stock enzyme solution contained 0.1% (w/v) Tween 80. The assay mixture without the enzyme was brought to 40 °C, and the reaction was started by the addition of the enzyme (up to 50 μL). After incubation for 10 min, the reaction was stopped by the addition of 300 μL 1 M Tris/HCl, pH 9.5; the mixture was then immediately chilled on ice. Fluorescence intensity changes in the reaction mixture (excitation 340 nm; emission 440 nm) were determined with a Shimadzu fluorescence spectrophotometer RF-5000. The blank did not contain the enzyme. The fluorescence intensity changes where known concentrations of the substrate were completely degraded by the addition of an excess amount of the collagenase under these assay conditions were also determined and were used for calculations of enzyme activity. The absorption coefficient of the purified enzymes was calculated from the amino-acid sequence [15] and used for calculation of k_{cat} values. Kinetic parameters and their standard errors were determined from the initial velocity data by nonlinear regression analysis [29]. The pH-dependence of kinetic parameters was determined as described above except that 0.1 M sodium acetate/0.1 M sodium phosphate was used as the buffer component and the pH was varied from 2.5 to 8.0; the buffering capacity was sufficient for the present enzyme assays. The wild-type enzyme, the mutants, and the IQF substrate (without added enzyme) were all stable under the conditions of these pH-dependent kinetic studies (pH 2.5–8.0, 40 °C for 10 min). However, the enzyme was unstable at pH 9 or higher. Thus, the enzyme reaction could be effectively terminated by the addition 1 M Tris/HCl, pH 9.5 (see above), even though the E78H/D164N mutant showed an optimum pH for catalytic activity at pH > 7. The graphical method of Siegel [30] was used to determine pK_a values from the $\log k_{cat}$ vs. pH and $\log k_{cat}/K_m$ vs. pH profiles.

Analysis of the ligation process of the E78H/D164N mutant

A 100-μL portion of 50 mM sodium acetate buffer, pH 4.0, containing the purified E78H/D164N mutant (the nicked form of the precursor, 55 μg; see above) was mixed with 400 μL 0.1 M Tris/HCl buffer, pH 7.3, and the mixture was incubated at 4 °C. At time intervals, an aliquot (15 μL) was withdrawn and mixed with an equal volume of 0.125 M Tris/HCl, pH 6.8, containing 10% (v/v) 2-mercaptoethanol, 4% (w/v) SDS, 10% (w/v) sucrose, and 0.004% (w/v) bromophenol blue, followed by heat treatment at 97 °C for 3 min. The sample (14 μL) was then analyzed by SDS/PAGE [21]. The pH-dependence of the ligation process (at 4 °C for 5 h) was analyzed as described above except that 0.1 M sodium acetate/0.1 M sodium phosphate was used as the buffer component for pH 2.5–7.4 (final pHs) and 0.1 M Tris/HCl buffer for pH 9.0. The intensities of the protein bands were quantified by densitometry, using a Shimadzu CS9000 apparatus (Shimadzu, Kyoto, Japan).

Acknowledgements

We are grateful to Dr Hong Guo, University of Tennessee, for his helpful comments and discussions. This research was supported in part by the Intramural Research Program of the NIH, National Cancer Institute, Center for Cancer Research, in part with Federal funds from the National Cancer Institute, NIH, under Contract No. NO1-CO-12400, and in part by NIH grant AI28571 to B.M.D. The content of this publication does not necessarily reflect the views or policies of the Department of Health and Human Services, nor does mention of trade names, commercial products, or organizations imply endorsement by the US Government.

References

1 Rawlings ND, Tolle DP & Barrett AJ (2004) MEROPS: the peptidase database. *Nucleic Acids Res* **32**, D160–D164.

2 Oda K, Sugitani M, Fukuhara K & Murao S (1987) Purification and properties of a pepstatin-insensitive carboxyl proteinase from a gram-negative bacterium. *Biochim Biophys Acta* **923**, 463–469.
3 Oda K, Takahashi T, Tokuda Y, Shibano Y & Takahashi S (1994) Cloning, nucleotide sequence, and expression of an isovaleryl pepstatin-insensitive carboxyl proteinase gene from *Pseudomonas* sp. 101. *J Biol Chem* **269**, 26518–26524.
4 Wlodawer A, Li M, Dauter Z, Gustchina A, Uchida K, Oyama H, Dunn BM & Oda K (2001) Carboxyl proteinase from *Pseudomonas* defines a novel family of subtilisin-like enzymes. *Nat Struct Biol* **8**, 442–446.
5 Wlodawer A, Li M, Gustchina A, Oyama H, Dunn BM & Oda K (2003) Structural and enzymatic properties of the sedolisin family of serine-carboxyl peptidases. *Acta Biochim Polon* **50**, 81–102.
6 Comellas-Bigler M, Fuentes-Prior P, Maskos K, Huber R, Oyama H, Uchida K, Dunn BM, Oda K & Bode W (2002) The 1.4 Å crystal structure of kumamolysin: a thermostable serine-carboxyl-type proteinase. *Structure* **10**, 865–876.
7 Wlodawer A, Li M, Gustchina A, Tsuruoka N, Ashida M, Minakata H, Oyama H, Oda K, Nishino T & Nakayama T (2004) Crystallographic and biochemical investigations of kumamolisin-As, a serine-carboxyl peptidase with collagenase activity. *J Biol Chem* **279**, 21500–21510.
8 Wlodawer A, Durell SR, Li M, Oyama H, Oda K & Dunn BM (2003) A model of tripeptidyl-peptidase I (CLN2), a ubiquitous and highly conserved member of the sedolisin family of serine-carboxyl peptidases. *BMC Struct Biol* **3**, 8.
9 Kraut J (1977) Serine proteases: structure and mechanism of catalysis. *Annu Rev Biochem* **46**, 331–358.
10 Dodson G & Wlodawer A (1998) Catalytic triads and their relatives. *Trends Biochem Sci* **23**, 347–352.
11 Robertus JD, Kraut J, Alden RA & Birktoft JJ (1972) Subtilisin: a stereochemical mechanism involving transition-state stabilization. *Biochemistry* **11**, 4293–4303.
12 Golabek AA, Wujek P, Walus M, Bieler S, Soto C, Wisniewski KE & Kida E (2004) Maturation of human tripeptidyl-peptidase I *in vitro*. *J Biol Chem* **279**, 31058–31067.
13 Comellas-Bigler M, Maskos K, Huber R, Oyama H, Oda K & Bode W (2004) 1.2 Å crystal structure of the serine carboxyl peptidase pro-kumamolisin: structure of an intact pro-subtilase. *Structure* **12**, 1313–1323.
14 Tsuruoka N, Isono Y, Shida O, Hemmi H, Nakayama T & Nishino T (2003) *Alicyclobacillus sendaiensis* sp. nov., a novel acidophilic, slightly thermophilic species isolated from soil in Sendai, Japan. *Int J Syst Evol Microbiol* **53**, 1081–1084.
15 Tsuruoka N, Nakayama T, Ashida M, Hemmi H, Nakao M, Minakata H, Oyama H, Oda K & Nishino T (2003) Collagenolytic serine-carboxyl proteinase from *Alicyclobacillus sendaiensis* strain NTAP-1: purification, characterization, gene cloning, and heterologous expression. *Appl Environ Microbiol* **69**, 162–169.
16 Stepanov VM, Strongin AY, Izotova LS, Abramov ZT, Lyublinskaya LA, Ermakova LM, Baratova LA & Belyanova LP (1977) Intracellular serine protease from *Bacillus subtilis*. Structural comparison with extracellular serine proteases-subtilisins. *Biochem Biophys Res Commun* **77**, 298–305.
17 Guo H, Wlodawer A & Guo H (2005) A general acid-base mechanism for the stabilization of a tetrahedral adduct in a serine-carboxyl peptidase: a computational study. *J Am Chem Soc* **127**, 15662–15663.
18 Carter P & Wells JA (1987) Engineering enzyme specificity by 'substrate-assisted catalysis'. *Science* **237**, 394–399.
19 Wlodawer A, Li M, Gustchina A, Dauter Z, Uchida K, Oyama H, Goldfarb NE, Dunn BM & Oda K (2001) Inhibitor complexes of the *Pseudomonas* serine-carboxyl proteinase. *Biochemistry* **40**, 15602–15611.
20 Oyama H, Hamada T, Ogasawara S, Uchida K, Murao S, Beyer BB, Dunn BM & Oda K (2002) A CLN2-related and thermostable serine-carboxyl proteinase, kumamolysin: cloning, expression, and identification of catalytic serine residue. *J Biochem (Tokyo)* **131**, 757–765.
21 Laemmli UK (1970) Cleavage of structural proteins during the assembly of the head of bacteriophage T4. *Nature* **227**, 680–685.
22 Davis BJ (1964) Disc Electrophoresis II. Method and application to human serum proteins. *Ann N Y Acad Sci* **121**, 404–427.
23 Otwinowski Z & Minor W (1997) Processing of X-ray diffraction data collected in oscillation mode. *Methods Enzymol* **276**, 307–326.
24 Navaza J (1994) *AMoRe*: an automated package for molecular replacement. *Acta Crystallogr* **A50**, 157–163.
25 Sheldrick GM & Schneider TR (1997) SHELXL: High-resolution refinement. *Methods Enzymol* **277**, 319–343.
26 Jones TA & Kjeldgaard M (1997) Electron-density map interpretation. *Methods Enzymol* **277**, 173–208.
27 Engh R & Huber R (1991) Accurate bond and angle parameters for X-ray protein-structure refinement. *Acta Crystallogr* **A47**, 392–400.
28 Cohen GE (1997) ALIGN: a program to superimpose protein coordinates, accounting for insertions and deletions. *J Appl Crystallogr* **30**, 1160–1161.
29 Leatherbarrow RJ (1991) Using linear and non-linear regression to fit biochemical data. *Trends Biochem Sci* **15**, 455–458.
30 Siegel IH (1975) *Enzyme Kinetics. Behavior and Analysis of Rapid Equilibrium and Steady-State Enzyme Systems* pp. 896–898. John Wiley & Sons, Inc, New York.